Chapter 4

Chaos Control in Simple Excitatory-Inhibitory Neural Network Models

Neurobiological studies have indicated that rapid transitions between chaotic and relatively more ordered states may be the key towards understanding how the brain performs cognitive tasks. This immediately suggests that methods of controlling chaos may be used to study similar phenomena in neural network models. In the work described in this chapter, control of chaotic behavior is investigated in chaotic neural network models. On imposition of control, transition of the network behavior from chaos to periodicity is observed. This has implications for both the explanation of observed neurobiological phenomena (e.g., olfactory hallucinations during epileptic seizures) as well as a more dynamic interpretation of associative recall performed by neural network models.

The next section reviews some existing techniques of chaos control which can drive a system from chaotic to ordered behavior. In Section 2, we analyze the physical mechanism of control in a chaotic neural pair, achieved through, either, a feedback to a system variable, or, through periodic forcing. Section 3 reports the results of applying control to a chaotic neural network comprising three pairs of excitatory and inhibitory neurons, while, in Section 4, the relevance of this type of research to explaining neurobiological phenomena is discussed. Finally, some observations on the possible applications of chaos control in neural computation are briefly mentioned.

4.1 Chaos control

One of the distinguishing features of chaotic attractors is that they have an infinite number of periodic attractors embedded within them. If the system state exists at any time on a region belonging to one of the periodic attractors then it will remain within it. However, as the attractors are unstable, when perturbed by noise, the system diverges away from the periodic orbit at an exponential rate. In a chaotic attractor, the system state may be, at any given time, infinitesimally close to any one of the infinite periodic attractors but due to the highly unstable nature of the periodic orbits, the periodicity is never manifested over a measurable period of time.

Ott, Grebogi and Yorke have used this feature of chaotic attractors to construct a general method of controlling chaos, i.e. to convert the chaotic behavior of a system to a time-periodic one [135, 161]. Their method (referred to as OGY method henceforth) achieves this control by making small, carefully chosen time-dependent perturbations of one of the parameters of the system. To obtain a periodic orbit, a local map around the desired attractor is constructed by the method of delay-coordinate embedding. In this method, the experimentally obtained time-series of a system is used to construct a $(n+1)$-dimensional (say) delay-coordinate vector, whose time-evolution can be plotted to give a 3-dimensional projection of the trajectory. It has been mathematically demonstrated that such a projection is a good approximation of the dynamical attractor of the relevant system in $(n + 1)$-dimensional space [138], [27]. The OGY control method relies upon the identification of saddle instabilities, i.e., unstable periodic points located on a surface having both stable and unstable directions. The system approaches the periodic point along a stable direction and diverges away from it along an unstable one. When the chaotic system state is in the neighborhood of the desired attractor, a perturbation is applied to a system parameter such that on the next iteration the system state falls on the stable direction. The state will then move towards the attractor in successive iterations. Using this principle, many physical systems exhibiting chaotic behavior has been subjected to control. However, one drawback of this method is that only low-period orbits can be stabilized, since, because of the exponential error magnification in chaotic systems, high-period stable orbits are extremely difficult to achieve by making only one correction in the long period. The OGY method has been used to control chaos in a biological neural network prepared from a hippocampal slice of a rat brain [155]. Using precisely timed electrical stimulation of the brain slice, the system was perturbed such that a trajectory coincided with a stable direction in the neighborhood of a periodic attractor. Thereafter the point moved towards the attractor with successive iterations and the resulting trajectories became periodic. In a similar way, anticontrol was achieved by perturbing a stable orbit, so that the next iterate falls close to the unstable direction, with a corresponding transition from periodic to chaotic behavior.

An alternative method of controlling chaos, called "occasional proportional feedback" (OPF), has been proposed by Hunt [93]. This allows stabilization of longer orbits than that possible through the OGY method. As higher period orbits visit most regions of the attractor, which correspond to different physical states of the system, it is desirable to have high-period orbits if one wishes to sample as many of the states as possible. In the OPF method, feedback is used to modulate the system parameter. The deviations of a chaotic variable within a specified window, centered about a specified value of a chosen system variable, are fed back to the system. By varying the control parameters, different periodic orbits are stabilized. A theoretical framework for this control mechanism has been sought to be developed by Carr and Schwartz [30].

Both the methods mentioned above apply the control signal to the system parameter. Feedback to the system variable, has also been applied to control chaotic systems with success. One such method [120] is based on the application of a periodic proportional feedback to the system variable, such that, every p time steps (say), the system is modified by means of a proportional feedback. As a result, an unstable periodic orbit, of period equal to a multiple of p is found to be stabilized. This method has been used to control the chaotic behavior of small, discrete neural networks [179], where the control is applied to one of the neurons, the others being free of direct control.

4.2 Controlling chaos in a neural pair

In this section we demonstrate two different ways of controlling the discrete-time chaotic dynamics of an excitatory-inhibitory neural pair. The first method is based on the application of proportional feedback to the system variable (instead of the system parameter, as in the OPF method) described above. The second method involves subjecting the neural pair to an external periodic stimulus.

4.2.1 System variable feedback method

To observe the effect of applying occasional proportional feedback to the system variable, let us consider the case of a neural pair whose dynamics is governed by piecewise linear activation functions. As already mentioned in Chapter 2, the behavior of a neural pair, with function parameters, $a = 4$ and $b = 2$, is identical to that of the "tent" map:

$$\begin{aligned} z_{n+1} &= 2z_n, \quad \text{for } 0 < z_n < 0.5, \\ &= 2(1 - z_n), \quad \text{for } 0.5 < z_n < 1, \end{aligned} \tag{4.1}$$

with the difference being that the phase space of the neural system is confined to the interval $[0, 0.5]$, while the tent map is defined in the unit interval $[0, 1]$. However, this distinction can be removed by suitable rescaling. We shall therefore focus on the tent map as the system to which the proposed control mechanism is applied.

The tent map, as defined above, is chaotic over the entire unit interval. The Lyapunov exponent of the system is $\lambda = \log_e 2 \simeq 0.693$, and the expansion of small perturbations among nearby trajectories is uniform throughout the interval. The results obtained for this specific case, are easily generalizable to maps with a globally uniform stretching rate, and, with slight modifications, to piecewise uniform stretching rates.

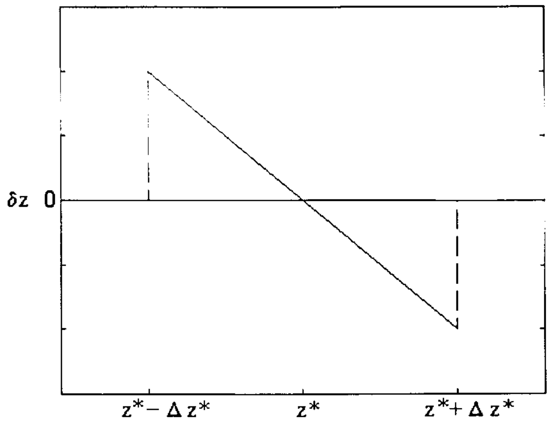

Figure 4.1: The input-output relation of the control signal, δz, with the control parameters, z^* and Δz^*. The feedback magnitude, α, gives the slope of the function.

If $z_{n+1} = \mathbb{F}(z_n)$ represent the system to be controlled (in the present case, $\mathbb{F}$ is given by Eqn. (4.1)), then the on applying control, we have the modified system:

$$z_{n+1} = \mathbb{F}(z_n) + \delta z_n, \tag{4.2}$$

where, δz_n, represents the control signal. For the proposed control method, the control signal is obtained by

$$\delta z_n = \alpha \mathcal{F}_{\Delta z^*}(z^* - \mathbb{F}(z_n)). \tag{4.3}$$

Here, z^* is the system state which is desired to be stabilized, α is a parameter governing the magnitude of feedback and $\mathcal{F}$ is a function, defined as,

$$\begin{aligned} \mathcal{F}_\mu(\xi) &= \xi, \text{ if } |\xi| < \mu, \\ &= 0, \text{ otherwise.} \end{aligned}$$

As is evident from the form of $\mathcal{F}$, the control signal is generated only on occasions when the system variable $z \in \mathbb{F}^{-1}(z^* \pm \Delta z^*)$ (see Fig. 4.1).

Let us now see the effect of the above control mechanism on the tent map. If $z_n = \mathbb{F}^{-1}(z^* + \Delta z)$, where $\Delta z < \Delta z^*$, then, on the next iteration, the system goes to

$$z_{n+1} = z^* + \Delta z + \alpha(z^* - z^* - \Delta z).$$

Now for the tent map, $\mathbb{F}^{-1}(z) = \frac{z}{2}$, so that,

$$\Delta z = 2z_n - z^*.$$

Therefore, one can write the resultant system dynamics, in the presence of control, as

$$z_{n+1} = 2z_n - 2\alpha z_n + \alpha z^*. \tag{4.4}$$

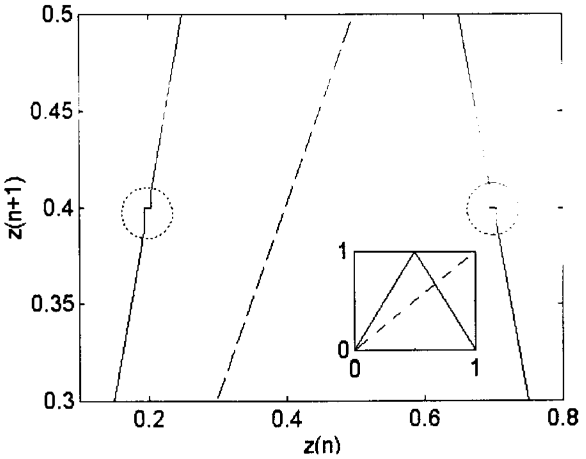

Figure 4.2: The effect of feedback control ($z^* = 0.4$, $\Delta z^* = 0.02$ and $\alpha = 1$) to the system variable of the tent map (inset), $\mathbb{F}$, is shown in a magnified view. The regions $\mathbb{F}^{-1}(z^*) \pm \Delta z^*$ have a slope of zero, the rest of the map remaining unchanged.

The above expression implies that, the slope of the map, in the region $\mathbb{F}^{-1}(z^* \pm \Delta z^*)$, has been modified to

$$\frac{dz_{n+1}}{dz_n} = 2(1-\alpha),$$

on the application of control. This is shown, for $z^* = 0.4, \Delta z^* = 0.02$ and $\alpha = 1$, in Fig. 4.2. Note that, the slope of the map is the system parameter governing the nature of the dynamics. This implies that the effect of feedback to the system variable is the same as local parametric perturbation around the desired region of the phase space to be controlled.

We shall now investigate the conditions under which a period-p cycle is stabilized by the control method. Let, the p-th iterate, $\mathbb{F}^p$, be the lowest order iterate of the map, to have a fixed point in the region $\mathbb{F}^{-1}(z^* \pm \Delta z)$. The stability of the fixed point is decided by the magnitude of its slope, m. In the case of the tent map,

$$m = 2^p(1-\alpha). \tag{4.5}$$

The p-th order cycle is stable only if $|m| < 1$, so that, by Eqn. (4.5), the critical value of α at which the cycle just becomes stable is:

$$\alpha_c = 1 - \frac{1}{2^p}. \tag{4.6}$$

For example, a fixed point can be stabilized for $\alpha > 0.5$, while a stable 2-cycle is obtained only for $\alpha > 0.75$, and similarly for higher order periodic cycles.

The time required for the system to converge to the stable state, on application of the control mechanism, is dependent upon Δz^*. The average time required for convergence can be obtained analytically in the case of the tent map. The extent of the region in which control is activated is $2\Delta z^*$. As the map is defined in the unit interval, the probability that a trajectory is in this region is also $2\Delta z^*$. If the system is in another region, the probability that it enters the control region is $2\Delta z^*(1-2\Delta z^*)$. Proceeding in this manner, the probability for the trajectory to enter the control region after n iterations, is given by

$$P(n) = 2\Delta z^*(1 - 2\Delta z^*)^n. \tag{4.7}$$

Therefore, the average time required for convergence is

$$< n >= \Sigma_{n=0}^{\infty} nP(n) = 2\Delta z^* \Sigma_{n=0}^{\infty} n(1 - 2\Delta z^*)^n. \tag{4.8}$$

This is evaluated as

$$< n >= \frac{(1 - 2\Delta z^*)}{2\Delta z^*}, \tag{4.9}$$

which, comes out to be $\simeq 49$, for $\Delta z^* = 0.01$. An example of a controlled transition from chaos to a period-2 cycle is shown in Fig. 4.3, for the control parameters: z^*=0.4, $\Delta z^* = 0.01$ and $\alpha = 1$. The control mechanism is turned on at $n = 50$ (indicated by an arrow "a") and the periodic cycle is stabilized quite rapidly (indicated by an arrow "b"). The bottom panel of Fig 4.3 shows the magnitude of the control signal, δz.

Since the control perturbation, δz, is a function of the neuron state, z_n, and a desired system state, z^*, the control method can be implemented as a network of excitatory-inhibitory neural pairs with suitable connection weights and activation function parameters (Fig. 4.4). The combination of a chaotic neural pair with a controlling neural system provides a neuromodule for stabilizing various periodic orbits, as suggested in [186]. Note that, an entire periodic sequence can be stabilized if only one of its members is known. Therefore, for a system with uniform stretching rate (e.g., the tent map), there is no necessity for obtaining a time-series to generate a control signal - a single stationary input is sufficient. The method has the further advantage of being extremely simple to implement, as compared to, say, the OGY method, which involves intensive calculations.

4.2.2 External periodic stimulation

Periodic cycles can also be stabilized by applying a periodic external input. This had been observed in the case of chaotic nonlinear oscillators evolving in continuous time [25]. Similar phenomena has been observed in our neural model.

For an excitatory-inhibitory neural pair, with activation functions of sigmoid nature, the effect of applying a periodic signal has been observed. As already mentioned in Chapter 3, for low-frequency signals, nonlinear resonance occurs. However, if the signal is of higher frequency, periodic orbits of various orders are stabilized. The reason for this phenomena is as follows.

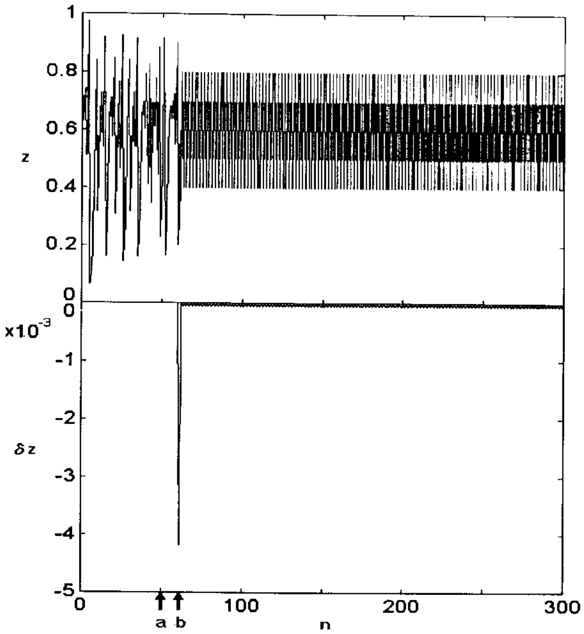

Figure 4.3: (Time series of the tent map subjected to control (top) and the magnitude of the control signal (bottom). The arrows a and b indicate the switching on of the control mechanism and the onset of controlled periodic cycles, respectively.

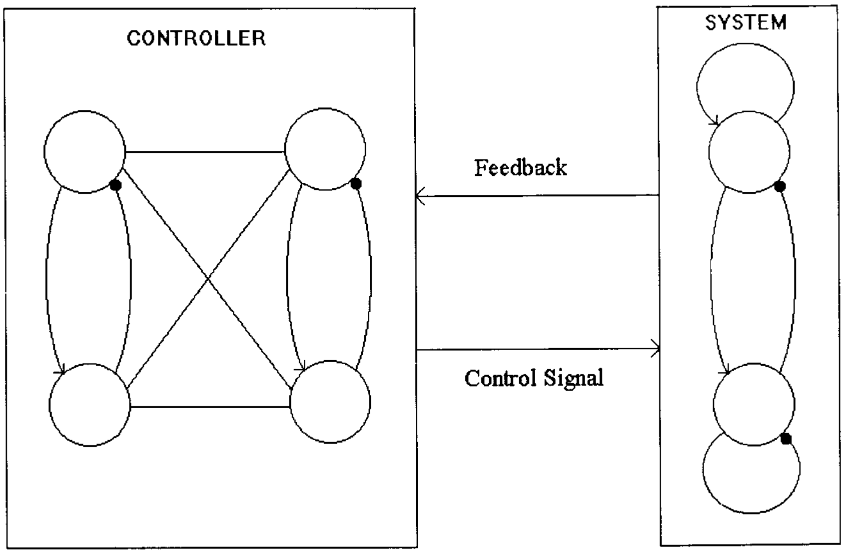

Figure 4.4: A biologically plausible mechanism for implementing the feedback control mechanism demonstrated for the tent map.

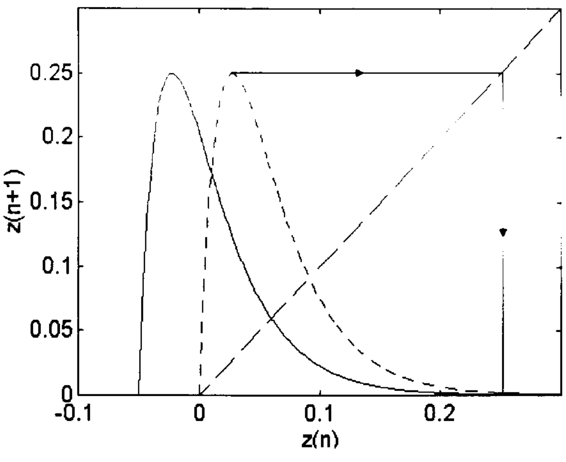

Figure 4.5: The map representing the dynamics of the excitatory-inhibitory neural pair ($a = 50, b = 25$) governed by sigmoid activation function subjected to control by a periodic external input of peak amplitude $\delta = 0.05$. The broken curve indicates the unperturbed map (F_1), while the solid curve indicates the shifted map (F_2) due to the periodic input.

Let the unperturbed map be chaotic in nature. On applying a periodic signal, the map is translated periodically, so that the slope at different points of the map is a function of time. Consider the case of a period-2 signal, which switches alternately between 0 and δ (Fig. 4.5). The trajectory from the critical point of the unperturbed map, F_1 (indicated by broken lines), iterates to the tail portion of the shifted map, F_2 (indicated by solid lines). Note that the slope, at this region, of the perturbed map, is much less than that of the original map. The stability of a period-2 cycle (z_1, z_2), is decided by the slope of the fixed point of the composite map, $F_1 * F_2$, given by:

$$m = \frac{dF_1}{dz}|_{z=z_1} \times \frac{dF_2}{dz}|_{z=z_2}.$$

Now, $|\frac{dF_2}{dz}|_{z=z_2} \ll 1 \Rightarrow |m| < 1$ (for sufficiently large δ), indicating the stabilization of the period-2 cycle.

4.3 Chaotic neural network model

We shall now consider a network comprising a larger number of elements for the purpose of controlling unstable periodic cycles. The present work has been done on an excitatory-inhibitory neural network model, which is a discrete-time version of a model proposed by Hayashi [80]. The system consists of N excitatory and N inhibitory elements, denoted by x_i and y_i, respectively (Fig. 4.6). The cells update

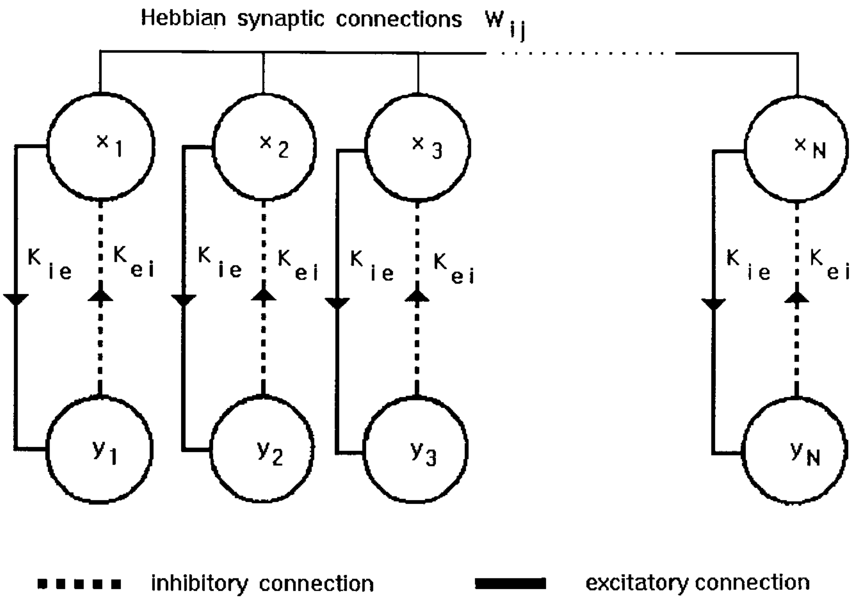

Figure 4.6: The oscillatory neural network model. Excitatory and inhibitory cells are labeled as x and y, respectively. W_{ij} represents the connection weights between the excitatory cells. K_{ei} is the strength of inhibitory connection from y to x and K_{ie} is the strength of excitatory connection from x to y.

their states in the $(n+1)$th iteration, according to the following transformations:

$$x_i(n+1) \;=\; G(\sum_{j=1}^{N} W_{ij}\; x_j(n) \;-\; K_{EI}\; y_i(n) \;+\; I_i(\omega)) \tag{4.10}$$

and,

$$y_i(n+1) \;=\; G(K_{IE}\; x_i(n) \;+\; I_i(\omega+\delta)) \tag{4.11}$$

where, $I(\omega)$ is an external periodic input or bias, δ is a phase difference between the inputs to x_i and y_i and, the function G is defined as,

$$G(z) \;=\; \frac{2}{\pi}\;\arctan(z/a) \tag{4.12}$$

a being the slope of the function. This parameter is analogous to 'temperature' in a physical system.

Thus, while excitatory cells are all connected to each other, inhibitory cells are connected only to the corresponding excitatory cells - K_{IE} being the weightage of the excitatory connection from x_i to y_i and K_{EI} being the inhibitory connection weightage from y_i to x_i. It is evident that x_i and y_i vary between +1 and -1. The activation values of the excitatory cells at time t, $x_i(t)$, is taken as the output of the network at that instant of time.

The synaptic connection weights W_{ij} between the excitatory cells, x_i, are evaluated by a modification of the standard Hebb rule,

$$W_{ij} \;=\; \frac{1}{N} \sum_{\mu} \xi_i^{\mu}\, \xi_j^{\mu} \;+\; \delta_{ij} \tag{4.13}$$

where ξ_i^{μ} is the ith component of the μth pattern vector being stored in the network and δ_{ij} is the Kronecker delta function.

It is easily seen that the pair of first-order difference equations (4-5) is equivalent to the second-order difference equation:

$$x_i(n+1) \;=\; G(\sum_{j=1}^{N} W_{ij}\, x_j(n) \;-\; K_{EI}\, G(K_{IE}\, x_i(n-1) \;+\; I_i(\omega+\delta)) \;+\; I_i(\omega)) \tag{4.14}$$

which resembles a Hopfield-like model with delay-dynamics.

4.3.1 Stability analysis

The stability of the fixed points of a single excitatory-inhibitory pair is investigated in this section. Let z^* denote a fixed point of the pair of evolution equations for x_i and y_i. The Jacobian in the neighborhood of the fixed point in the absence of any external input is given by

$$\mathrm{J} \;=\; \begin{vmatrix} G'(z)|_{z=z^*} W_{ii} & G'(z)|_{z=z^*} K_{EI} \\ G'(z)|_{z=z^*} K_{IE} & 0 \end{vmatrix} \tag{4.15}$$

where $G'(z)$ is the derivative of $G(z)$ w.r.t. z.

The eigenvalues are given by the solution of the equation

$$\mathrm{Det} \;|\; \mathrm{J} \;-\; \lambda\, \mathrm{I} \;|\; = \; \mathbf{0} \tag{4.16}$$

where I is the identity matrix. This equation can be reduced to

$$\lambda^2 \;-\; \mathrm{Tr\ J}\, \lambda \;+\; \mathrm{Det\ J} \;=\; 0 \tag{4.17}$$

Thus,

$$\lambda_{1,2} \;=\; \frac{\mathrm{Tr\ J} \;\pm\; \sqrt{(\mathrm{Tr\ J})^2 \;-\; 4\ \mathrm{Det\ J}}}{2} \tag{4.18}$$

For $(\mathrm{Tr\ J})^2 - 4\,\mathrm{Det\ J} \geq 0$ the solutions eventually converges to the fixed point, which is thus stable. Evaluating J , $\mathrm{Tr\ J} \;=\; G'(z)|_{z=z^*}\, W_{ii}$ and $\mathrm{Det\ J} \;=\; (G'(z)|_{z=z^*})^2\, K_{IE}\, K_{EI}$. As $G'(z) \;=\; \frac{2\,a}{\pi\,(a^2+z^2)}$, the eigenvalues are given by,

$$\lambda_{1,2} \;=\; \frac{2\,a}{\pi\,(a^2+z^{*2})}\;(\,W_{ii} \;\pm\; \sqrt{W_{ii}^2 \;-\; 4\,K_{EI}\,K_{IE}}) \tag{4.19}$$

According to Eqn. (4.13), $W_{ii} = 2$. Therefore, the condition for stability of the fixed point is $K_{EI}\, K_{IE} \;\leq\; 1$. If this condition is not satisfied, all the fixed points of the second-order difference equation become unstable giving rise to periodic orbits.

4.3.2 Simulation results

For the present work, a network with N = 3 was used for carrying out computer simulations. The number of cells was kept low for ease of graphical analysis. The pattern vectors chosen for storage in the network were :

$$\xi^1 = (\ 1\ \ 1\ \ 1),\ \xi^2 = (\ 1\ \ -1\ \ -1),\ \xi^3 = (\ -1\ \ -1\ \ 1)$$

The memory patterns are, therefore, vertices of a cube, $-1 \leq x_i \leq 1$ (i=1,2,3). After evaluating the weight matrix, the network was made to evolve from a randomly chosen initial value. The initial states were taken as $x_i(0) = I_i$ and $y_i(0) = 0$. As pointed out above the condition for oscillations in a single excitatory-inhibitory pair is $K_{EI}\ K_{IE}\ \geq 1$. The system thus corresponds to three oscillators weakly coupled together through connection strengths $\sim$ **O** $(\frac{1}{N})$. If these three oscillators have independent periods of oscillations then, according to the results of Li and Yorke [110], the system is capable of chaotic behavior.

The simulation was carried out for the following set of parameters: $K_{EI} = 2.0$, $K_{IE} = 2.0$ and $a = 0.1$. An external sinusoidal input which completed one period every 300 iterations of the network with $\delta = 0$ was used to stimulate the network. The system showed chaotic activity when the input pattern vector was very different from any of the stored pattern vectors. The 3-dimensional plot of the trajectory of the network state in state space is shown in Fig. 4.7, while Fig. 4.8 shows the variation of the average activation of the excitatory cells with iteration number along with the corresponding logarithmic spectral density.

Another performance parameter to be noted is the overlap of the output of the network at a given time with each of the stored patterns. This is defined for the μth pattern vector at the nth iteration as

$$m^{\mu}(n) \ = \ \frac{1}{N} \sum_{i=1}^{N} x_i^{\mu}(n)\ \xi_i^{\mu} \qquad (4.20)$$

In Fig. 4.9 the overlap values are plotted against the number of iterations, for each of the three ξ^{μ}.

This chaotic system was then subjected to control by modulating the amplitude of the external periodic input. The resulting system, starting from the same initial conditions and network parameters as in the previous chaotic case, showed a time-series repeating every 15 iterations, after the initial transients had died away. The trajectory of the system state over time in Fig. 4.10 shows a simple periodic orbit. Regular periodic behavior is clearly manifested in the plot of the average excitatory cell activation and the corresponding logarithmic spectral density curve in Fig. 4.11.

The overlap vs. iterations diagram in Fig. 4.12 shows that the network periodically comes close to each of the three stored patterns. Thus, on imposing control, the system state exhibits periodicity quite clearly.

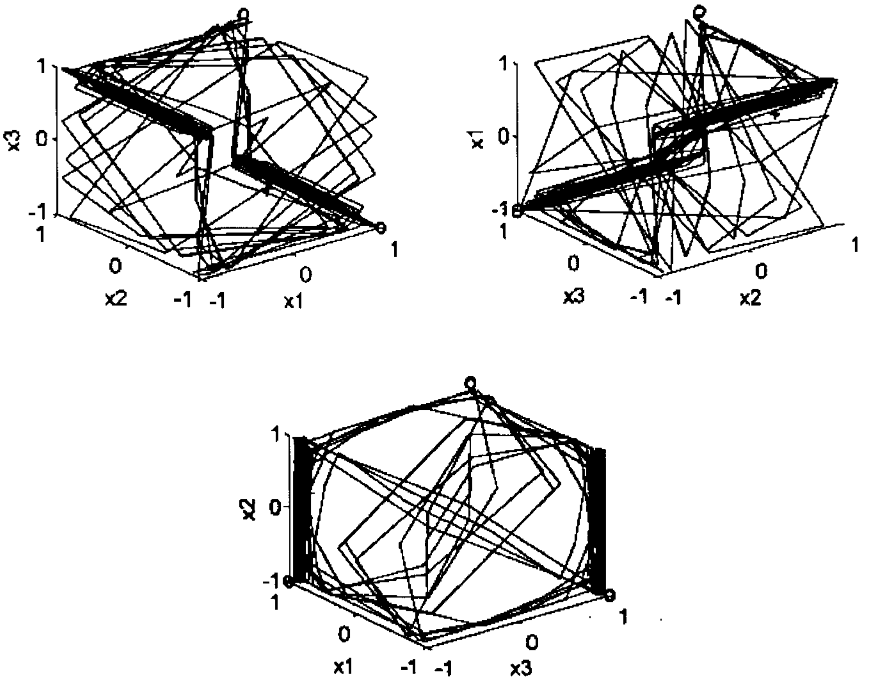

Figure 4.7: Trajectory of the network output in the chaotic state ($K_{ei} = 2.0$, $K_{ie} = 2.0$). The activation values for the cells $x(1)$, $x(2)$ and $x(3)$ are plotted along the three axes. The circles represent the locations of the stored patterns and the plus sign indicate the location of the input pattern.

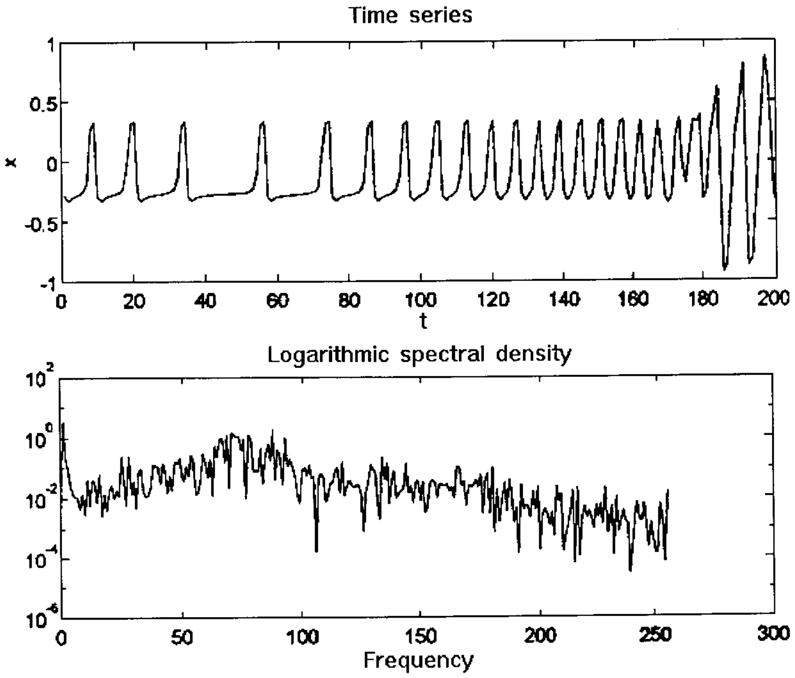

Figure 4.8: Temporal evolution of the average activation value of the excitatory cells in the chaotic state and the corresponding logarithmic spectral density.

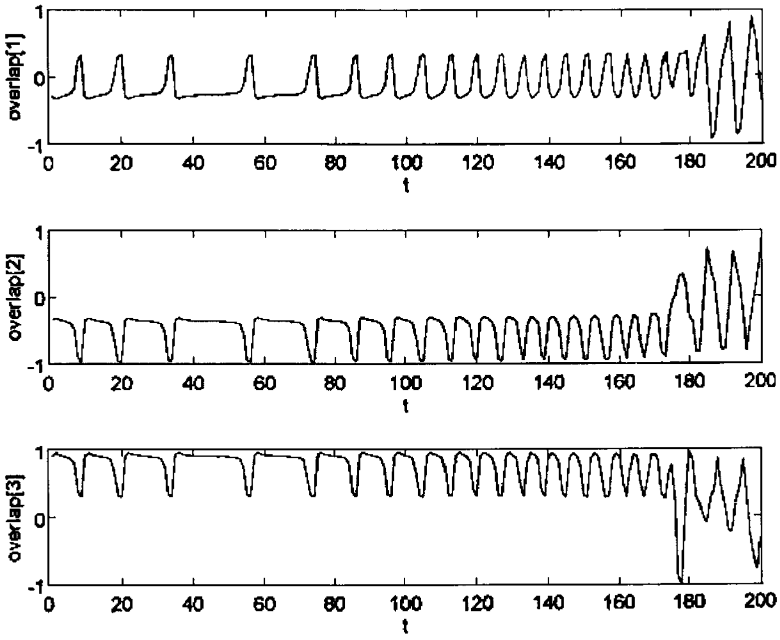

Figure 4.9: Temporal evolution of the overlap of the network output with the stored patterns in the chaotic state.

4.4 Neurobiological implications

The modeling of neurobiological chaos and its subsequent control to produce periodic behavior, points out several possible avenues for research aimed at understanding how the brain works. As Freeman has already pointed out [177], chaos is omnipresent in the brain - demonstrably so, in the somatosensory and the olfactory cortices. It has been suggested that the quiescent state of the brain is chaos, while during perception, i.e. when attention is focused on any sensory stimuli, brain activity becomes more periodic. From this perspective, the periodic orbits observed in the controlled state of the network model can be interpreted as specific memories. If the different spatio-temporal patterns stored in memory are identified with the infinite number of unstable periodic attractors that are embedded in the chaotic attractor, then the transition from quiescence to attention can be interpreted as the controlling of chaos to give rise to periodic behavior, culminating in the identification of the sensory stimulus that has been received. This control, of course, is not imposed by any external agency, but is an emergent property of the brain.

This identification is also indirectly supported by the clinical observations of hallucinations that are prevalent during sensory epileptic seizures [2]. Complex visual hallucinations are usually due to an epileptic focus in the posterior part of the temporal lobe, near its junction with the occipital lobe. Often the hallucinatory visual images are distorted, being too small or too large or unnaturally arranged. More

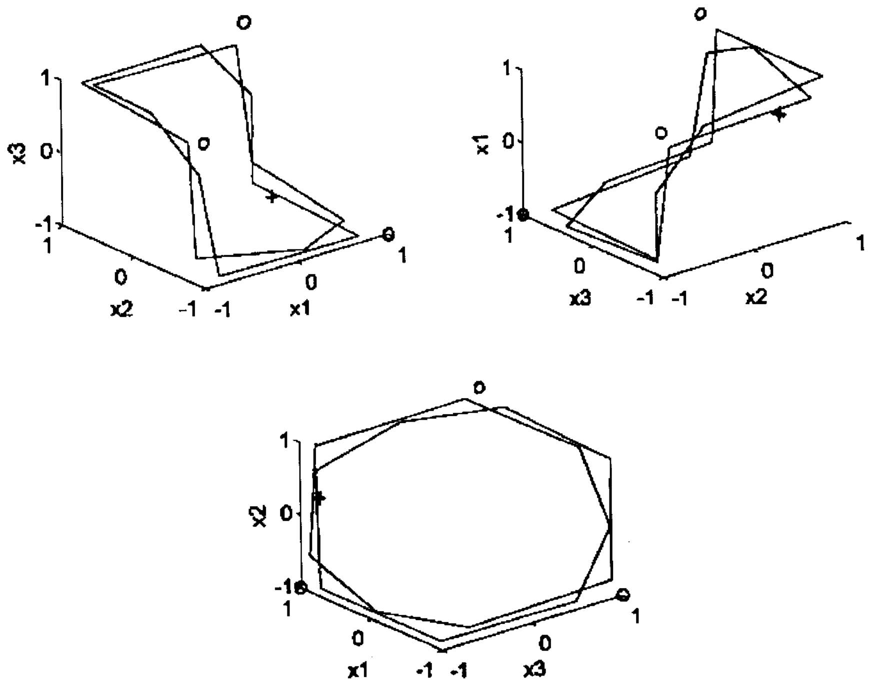

Figure 4.10: Trajectory of the network output in the controlled state for the same set of network parameters and input pattern as in Fig. 7.

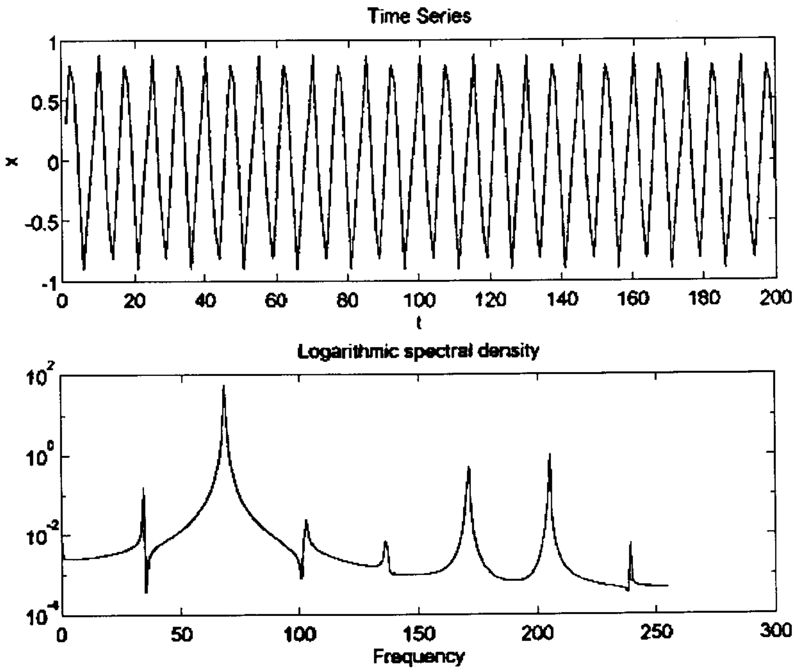

Figure 4.11: Temporal evolution of the average activation value of the excitatory cells in the controlled state and the corresponding logarithmic spectral density.

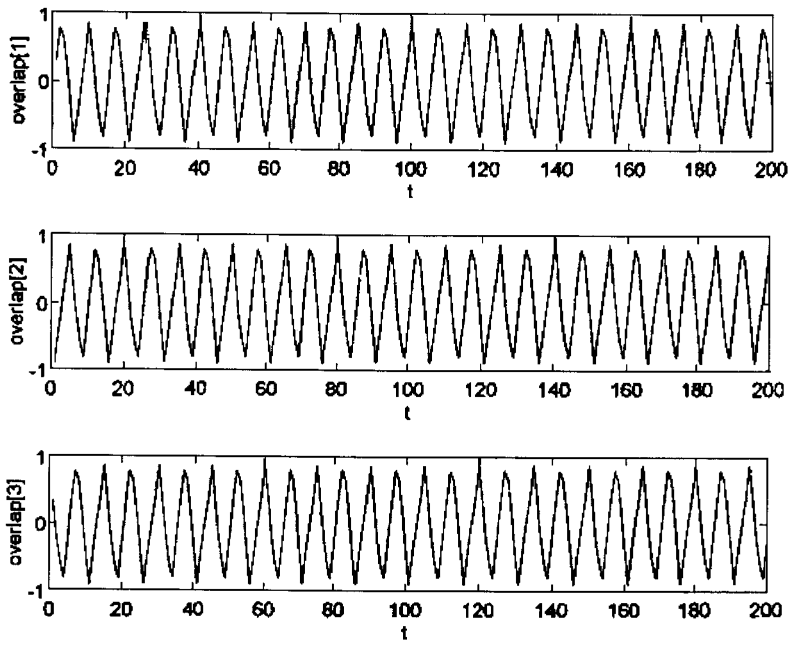

Figure 4.12: Temporal evolution of the overlap of the network output with the stored patterns in the controlled state.

striking is the case of olfactory hallucinations, that are often associated with disease of the inferior and medial parts of the temporal lobe, usually in the region of the hippocampal convolution. Commonly, the hallucinatory smell is thought by the subjects to come from some place in the environment and is described as disagreeable or foul, although otherwise unidentifiable. This can be explained in terms of the proposed picture of brain function by noting that during epilepsy, undesired control of the chaotic activity of the brain occurs as a result of the highly synchronized electrical stimulation of large parts of the brain. The stabilizing of an undesired periodic attractor results in the erroneous recognition of a sensory stimuli even when such a stimuli is absent from the immediate environment of the epileptic subject.

4.5 Discussion

In this investigation, we have confined our attention to small networks for convenience of analysis. The extension of the control methods to the situation of spatiotemporally extended systems [92] is a challenging task for the future.

The traditional neural network paradigm has been so far dominated by dynamics governed by a multitude of fixed point attractors [8]. Each such attractor is identified with a specific pattern which is desired to be classified appropriately and/or recalled associatively. But limitations of neural networks designed according to this prescription, as well as, recent neurobiological research, is now forcing this "fixed-point" approach to be replaced by a more dynamic interpretation of how cognitive tasks may actually be performed in the brain.

The use of chaos control can improve the performance of neural network models for processing information. The possibility of embedding an enormous amount of dynamic patterns (e.g., moving images, pieces of music, etc.) in a chaotic neural network and their systematic recognition will widen the scope of applications of neurocomputers. Rapid switching between various unstable periodic cycles, without large changes in the system dynamics, can be of use in tasks such as storing information and pattern classification. Temporal sequences can be associated with the unstable periodic attractors by suitable learning rules and then recalled on presentation of suitable stimulus as input to the network. The convergence to the stored patterns will be extremely rapid owing to the chaotic dynamics governing the network.

Although control of chaos (by the OGY method) has been demonstrated in the brain [155], it is still not clear whether a similar process is actually used in nature. In this situation, the investigation of different control processes in simple, biologically plausible neural models, can give us an insight on the possible functional role of such phenomena in the actual neurobiological situation.